

An Approach for Efficient Numerical Integration of the Sommerfeld Type Integrals Pertinent to the Microstrip Surface Green's Function

Ikguen Choi* *Regular Members*

Microstrip 표면 Green함수에 관한 Sommerfeld 형 적분들의 효과적인 수치 적분법

正會員 崔 翼 權*

ABSTRACT

An approach is presented for efficient numerical integration of the Sommerfeld type integrals pertinent to the microstrip surface Green's function arising in the problem of an electric current point source on an infinite planar grounded dielectric substrate. This approach, valid for both lossless and lossy dielectric substrates, is based on the deformation of the integration contour via a coordinate transformation and Cauchy's residue theory, and identifies clearly the effects of surface waves. Its useful application is in a rigorous moment method analysis of microstrip antenna arrays and microstrip guided wave structures. The efficiency and the usefulness of the present approach are emphasized through some numerical calculations of the impedance matrix elements with associated CPU times.

I. Introduction

For a rigorous moment method (MM) analysis of microstrip antenna arrays and microstrip guided wave structures, the key step is the computation of the impedance matrix elements. This involves repeated evaluation of the Sommerfeld type integrals pertinent to the electric field on air-dielectric interface which is excited by a

transverse electric point current source located on an infinite grounded dielectric slab. Evaluation of these infinite integrals is rather time-consuming due to the slow decay and oscillatory nature of the integrands. Also, the pole singularities which may exist along or very close to the path of integration cause additional difficulties. Thus, evaluation of the impedance matrix elements can be numerically inefficient.

Several integration techniques are already available in [1,2] for rapid and accurate evaluation of these integrals. However, it is noticed

*韓國電子通信研究所
Electronics and Telecommunications Research Institute
論文番號: 93-15 (接受1992. 10. 7)

that these techniques are valid only for the case of lossless dielectric substrates. The present approach introduced in this paper is valid for both lossless and lossy cases. This approach first employs the polar coordinate transformation $k\rho = k_1 \sin \xi$ (k_1 is the free space wave number) to transform the Sommerfeld type integrals in the complex $k\rho$ -plane into the complex ξ -plane. Then, via application of Cauchy's residue theory in the complex ξ -plane, the original contour of integration is deformed into a contour which is chosen in such a way that the resulting alternative expression of each Sommerfeld type integral does not include the numerical difficulties as mentioned before and converges quickly. Thus, by employing the alternative representations developed here for the Sommerfeld type integrals one can perform the rigorous MM solution in a highly efficient manner.

The electromagnetic fields due to a point source in the problem geometry is presented in terms of the Sommerfeld type integrals in Section II. In section III, a new approach which leads to efficient evaluation of these integrals is presented. In Section IV, some numerical calculations of the impedance matrix elements with associated CPU times are presented to illustrate the efficiency of the present approach. In the following, the time convention $\exp(j\omega t)$ is assumed and suppressed.

II. Field Expressions in Terms of Sommerfeld Type Integrals

It has been shown^[1,2,3] that the solution for the

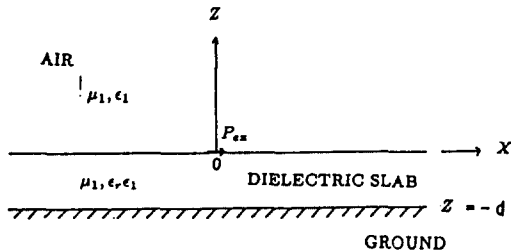


Fig. 1. \hat{x} -directed electric dipole on an infinite grounded dielectric slab.

fields excited by a \hat{x} -directed electric point current source on an infinite grounded dielectric slab (see Figure 1) can be derived in terms of two magnetic vector potential components A_x and A_z , and that the following representations for vector potential components satisfy the Maxwell's equations and the required boundary conditions : for $z \geq 0$,

$$A_x = \frac{\mu_1}{2\pi} \int_0^x \frac{k_\rho e^{-jk_{z1}z} J_0^{(2)}(k_\rho \rho)}{D_{TE}} dk_\rho; \quad (1)$$

$$A_z = -\frac{\mu_1}{2\pi} (\epsilon_r - 1) \cos\phi \int_0^x \frac{k_\rho^2 e^{-jk_{z1}z} J_1^{(2)}(k_\rho \rho)}{D_{TE} D_{TM}} dk_\rho; \quad (2)$$

where

$$\begin{aligned} \rho &= \sqrt{x^2 + y^2} & \cos\phi &= x/\rho \\ D_{TE} &= jk_{z1} + k_{z2} \cot(k_{z2}d) & D_{TM} &= j\epsilon_r k_{z1} - k_{z2} \tan(k_{z2}d) \\ k_{z1} &= \sqrt{k_1^2 - k_\rho^2}, \text{Re}(k_{z1}) > 0, \text{Im}(k_{z1}) < 0 \\ k_{z2} &= \sqrt{\epsilon_r k_1^2 - k_\rho^2}, \text{Re}(k_{z2}) > 0, \text{Im}(k_{z2}) < 0 \end{aligned} \quad (3)$$

The electric fields in free space ($z > 0$) are then given by

$$\bar{E} = \frac{-j}{\omega\mu_1\epsilon_1} (k_1^2 \bar{A} + \nabla\nabla \cdot \bar{A}).$$

The conditions for the transverse wave number k_{z1} in (3) are required since A_x and A_z represent outward-propagating or attenuated waves. However, the choice of sign of k_{z2} in (3) is not mandatory since $k_{z2}\cot(k_{z2}d)$ and $k_{z2}\tan(k_{z2}d)$ are even functions of k_ρ .

The Sommerfeld type integrals appearing in the above are time-consuming to evaluate due to the slow convergence of these integrals especially when the source and field points are on the dielectric surface ($z=0$): this case is of special interest in the MM solution of the microstrip problem. Several techniques for the lossless dielectric case have been introduced in [1,2] to reduce the computational time required in the evaluation of the Sommerfeld type integrals. In the following section, a quite differ-

ent approach is presented for efficient evaluation of the Sommerfeld type integrals as it is valid for both lossless and lossy cases.

III. An Approach for Efficient Evaluation of the Sommerfeld Type Integrals

Since the same approach is valid for both A_x and A_z , for convenience, let us consider A_x only to illustrate the present approach. This approach begins by deriving its alternative form in which the integration over k_ρ extends from $-\infty$ to $+\infty$. Upon introducing

$$J_q(t) = \frac{1}{2} [H_q^{(1)}(t) + H_q^{(2)}(t)] \quad (5)$$

where $H_q^{(1,2)}$ is the Hankel function of the first (second) kind of order q and argument t , one may write the representation (1) as

$$A_x = \frac{\mu_1}{4\pi} \int_0^\infty \frac{k_\rho e^{-jk_{z1}z} H_0^{(1)}(k_\rho \rho)}{jk_{z1} + k_{z2} \cot(k_{z2}d)} dk_\rho + \frac{\mu_1}{4\pi} \int_0^\infty \frac{k_\rho e^{-jk_{z1}z} H_0^{(2)}(k_\rho \rho)}{jk_{z1} + k_{z2} \cot(k_{z2}d)} dk_\rho. \quad (6)$$

The exponential terms in the expression of A_x will be eliminated from this point on, since we are specifically interested in the case where the field point is also on the dielectric surface ($z=0$). Applying the change of variables :

$$k'_\rho = k_\rho e^{-j\pi} \quad (7)$$

in the integrand of the first integrals in (6) and then using the relations

$$H_\rho^{(1)}(te^{j\pi}) = -e^{-j\rho\pi} H_\rho^{(2)}(t) \quad (8)$$

yields the following alternative form :

$$A_x = \int_{-\infty}^{\infty} F(k_\rho) H_0^{(2)}(k_\rho \rho) dk_\rho \quad (9)$$

where

$$F(k_\rho) = \frac{\mu_1}{4\pi} \frac{k_\rho}{jk_{z1} + k_{z2} \cot(k_{z2}d)} \quad (10)$$

In the complex k_ρ plane, the integrand in (9) is a multiple-valued function of k_ρ because of the double-valued function k_{z1} and the multiple-valued function $H_0^{(2)}(k_\rho \rho)$. However, for our intention to deform the original integration path, it is necessary to have the integrand single-valued in the whole complex k_ρ plane. It is found to be sufficient for this purpose to introduce two sheets of complex k_ρ plane which are connected by the branch cuts shown in Figure 2.

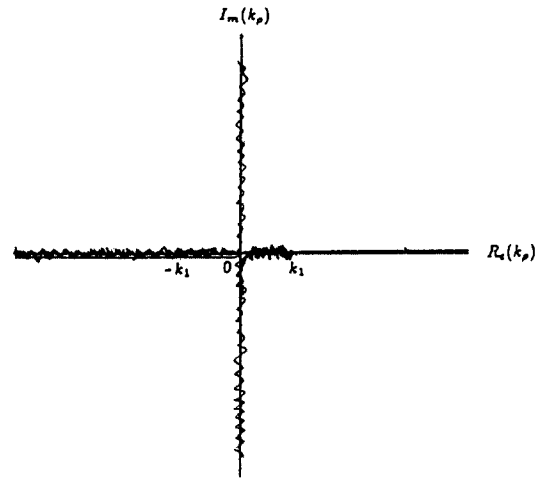


Fig. 2. Contour of integration and branch cuts in the complex k_ρ plane.

The branch cuts with the branch points at $k_\rho = \pm k_1$ (k_1 is assumed to be real) are introduced to ensure the single-valuedness of the double-valued function k_{z1} and are chosen as in this figure so that $Im(k_{z1})$ is negative on the top sheet and positive on the bottom sheet. The branch cut along the negative real axis is introduced to ensure the single-valuedness of the Hankel function.

It seems convenient to remove the branch cut singularities due to k_{z1} by means of the following polar transformations

$$\begin{aligned} k_\rho &= k_1 \sin \xi \\ k_{z1} &= k_1 \cos \xi \end{aligned} \quad (11)$$

where

$$\xi = u + jv \quad (12)$$

Then, A_x transformed into the complex ξ plane is

$$A_x = \int_{c_\xi} [F(k\rho)] k\rho = k_1 \sin \xi \cdot H_0^{(2)}(k_1 \rho \sin \xi) d\xi$$

$$kz_1 = z_1 \cos \xi \quad (13)$$

where c_ξ denotes the transformed original contour of integration and is shown in Figure 3.

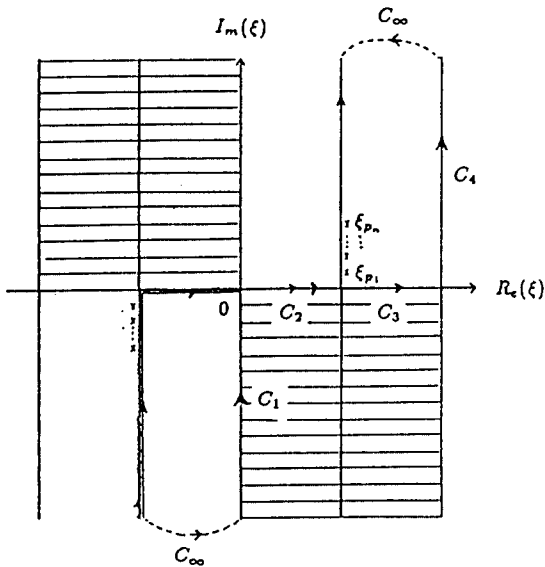


Fig. 3. The complex ξ plane. C_ξ represents the original contour transformed into the complex ξ plane. The regions unshaded and shaded with horizontal lines correspond to the top sheet where $I_m(kz_1) < 0$ and the bottom sheet where $I_m(kz_1) > 0$, respectively, in the complex $k\rho$ plane.

For analytical details involved in this transformation, one may refer to [4,5]. Now, in Figure 3, considering a closed contour which consists of the contour c_ξ and five additional contours C_1 , C_2 , C_3 , C_4 , and C_∞ it is clear, via Cauchy's residue theory, that the integral along the contour c_ξ is the

same as the sum of that along the other contours and the residues at the poles ξ_{pi} ($i=1, \dots, n$) enclosed by the closed contours since the integrand is regular in the region bounded by the closed contour except for the finite number of poles. Notice that the poles are always inside the closed contours, even though their locations are changed depending upon the loss tangent of the dielectric substrate. Combining the contributions of the contours C_1 , C_4 and C_2 , C_3 to the integral separately with a few algebraic modifications (the contribution of C_∞ is zero) and then introducing new variables t and λ via the transformations

$$t = \sinh v \quad (14)$$

and

$$\lambda = \sin u \quad (15)$$

yields an alternative expression for A_x as follows :

$$A_x = -2\pi j \sum_{i=1}^n R_i$$

$$+ \frac{\mu_1 k_1}{\pi^2} \int_0^\infty \frac{\sin^2(k_1 d \sqrt{\epsilon_r + t^2} t \sqrt{1+t^2} K_0(k_1 \rho t) dt}{(\epsilon_r + t^2) \cos^2(k_1 d \sqrt{\epsilon_r + t^2}) + (1+t^2) \sin^2(k_1 d \sqrt{\epsilon_r + t^2})}$$

$$- j \frac{\mu_1 k_1}{2\pi} \int_0^1 \frac{\sin^2(k_1 d \sqrt{\epsilon_r + \lambda^2} \lambda \sqrt{1+\lambda^2} K_0(k_1 \rho \lambda) d\lambda}{(\epsilon_r - \lambda^2) \cos^2(k_1 d \sqrt{\epsilon_r - \lambda^2}) + (1-\lambda^2) \sin^2(k_1 d \sqrt{\epsilon_r - \lambda^2})} \quad (16)$$

where R_i represents the residue of function $F(k\rho)$ $H_0^{(2)}(k\rho)$ at the i^{th} pole ($i=1, \dots, n$) and $K_0(\rho t)$ is a zero-order modified Bessel function of the second kind with argument ρt . For numerical evaluation of the infinite integral in (16), one can reduce it to the finite integration by ignoring the tail of the integrand since the modified Bessel function decays very rapidly. Finally, the following alterna-

tive expression is obtained for the efficient computation of the Sommerfeld type integral (1) :

$$\begin{aligned}
 A_x = & -2\pi j \sum_{i=1}^n R_i \\
 & + j \frac{\mu_1 k_1}{2\pi} \int_0^{t_c} \frac{\sin^2(k_1 d \sqrt{\epsilon_r + t^2} t \sqrt{1+t^2} K_0(k_1 \rho t) dt}{(\epsilon_r + t^2) \cos^2(k_1 d \sqrt{\epsilon_r + t^2}) + (1+t^2) \sin^2(k_1 d \sqrt{\epsilon_r + t^2})} \\
 & - j \frac{\mu_1 k_1}{2\pi} \int_0^1 \frac{\sin^2(k_1 d \sqrt{\epsilon_r + \lambda^2} \lambda \sqrt{1+\lambda^2} H_0^{(2)}(k_1 \rho \lambda) d\lambda}{(\epsilon_r - \lambda^2) \cos^2(k_1 d \sqrt{\epsilon_r - \lambda^2}) + (1-\lambda^2) \sin^2(k_1 d \sqrt{\epsilon_r - \lambda^2})}
 \end{aligned}
 \tag{17}$$

where

$$t_c = \frac{1}{k_1 \rho} (-m \ln_{10} 10 + \ln k_1 \rho) \text{ for } \epsilon < 10^{-m}. \tag{18}$$

ϵ and t_c in (18) denote a truncation error and a corresponding truncation point, respectively (see Appendix A).

Unlike the conventional Sommerfeld type integral (1), the integrands in (17) do not have pole singularities. Also, the zeroes of the integrands located on each finite integration interval, $0 \leq t \leq t_c$ and $0 \leq \lambda \leq k_1$, are found easily from the zeroes of the sinusoidal and Hankel functions in each denominator. Each sub-integration between the zeroes can be evaluated precisely by a rule like a Gaussian quadrature formula. This ensures the accuracy of the involved numerical integration for any dielectric constant and dielectric thickness (electrical), and this is one of the main reasons why the particular contours as shown in Figure 3 were chosen among infinitely many possible contours.

IV. Numerical Examples

One of the useful applications of the present method is in the calculation of impedance matrix elements for the moment method analysis of

microstrip patch antenna arrays. Thus, in this section, some numerical calculation of the impedance matrix elements with associated CPU times are presented to illustrate the accuracy and the efficiency of the present approach. Tables 1-3 show the self and mutual impedances between two \hat{x} -directed entire domain expansion modes. L and W denote the length and the width of the two identical modes, respectively. In each table, x and y represent the separation in meters between centers of each mode along the x -axis and the y -axis, respectively.

The second and third columns represent the nu-

Table. I

$$\begin{aligned}
 f = 4800 \text{ MHz, } \epsilon_r = 2.45, \quad D = 0.000787m \\
 L = 0.02296m, \quad W = 0.01744m
 \end{aligned}$$

x	y	Present Approach	PWST
0	0.	.323+j4.82	.323+j4.82
0	.0375	-.019-j.048	-.019-j.045
0	.075	.030+j.008	.030+j.006
0	.1125	-.020+j.009	-.020+j.010
0	.15	.008-j.015	.008-j.015

Table. II

$$\begin{aligned}
 f = 4800 \text{ MHz, } \epsilon_r = 2.45, \quad D = 0.003175m \\
 L = 0.02296m, \quad W = 0.01744m
 \end{aligned}$$

x	y	Present Approach	PWST
0	0.	5.95+j21.1	5.95+j21.0
0	.0375	-.613-j.592	-.613-j.533
0	.075	.646-j.143	.646-j.175
0	.1125	-.276+j.430	-.276+j.435
0	.15	-.078-j.418	-.078-j.402

Table. III

$$\begin{aligned}
 f = 300 \text{ MHz, } \epsilon_r = 12.8, \quad D = 0.06m \\
 L = 0.1074m, \quad W = 0.15m
 \end{aligned}$$

x	y	Present Approach	PWST
0	0.	9.21+j2.79	9.21+j3.933
0	.5	-4.25+j1.51	-4.25+j1.55
.5	.0	.486-j1.77	.486-j1.76
.5	.5	.283+j.75	.283+j.74

merical results calculated by employing the present approach for efficient evaluation of the Sommerfeld type integrals (refer to^[3] for detailed impedance representations) and the plane-wave spectral technique (PWST) widely used in literature for MM analysis of microstrip array antennas,^[6] respectively. They agree with each other, as expected. As is known,^[6,7] the accuracy of the plane-wave spectral representation depends upon a careful choice of the point at which the infinite integral is terminated, an accurate determination of the pole location and again, a careful choice of the Cauchy's principal value. The number of sampling points over integration must also be carefully chosen since the number of oscillation of the integrand increases with the separation between expansion modes.^[7]

In comparison to the PWST technique, impedance calculation via the present approach is about 10~20 times faster and evaluation of the impedances in Tables 1, 2, and 3 takes about 2 minutes, 2-2/3 minutes and 5 minutes of CPU time on a VAX 11/750, respectively. For the self-impedances alone, it takes about 25 seconds, 53 seconds, and 2 minutes and 10 seconds, respectively.

Notice that the alternative expressions of the Sommerfeld type integrals are computed in actual calculation by employing 12-point Gaussian quadrature formula for integration of each sub-interval whose end points are adjacent zeroes of the integrand and that the number of sub-intervals increase when the dielectric constant and the thickness increase. Thus, longer CPU times are required for higher dielectric constant and thicker dielectric substrate.

V. Conclusion

In this paper, an approach has been presented for the efficient evaluation of conventional Sommerfeld type integrals pertinent to the electric field on the air-dielectric interface produced by an arbitrary directed electric current point

source located on an infinite grounded dielectric slab. This approach involves the deformation of the integration contour via Cauchy's residue theory and is valid for both lossless and lossy dielectric substrate cases. CPU times taken on a VAX 11/750 for some numerical calculations of the self-and mutual-impedances between entire domain expansion modes are shown to be about 10 to 20 times faster than the conventional plane-wave spectral method.

Even though the present approach is applied here for the single-layered planar microstrip geometry, it is believed that the same approach can be applied for the multi-layered geometry.

Acknowledgement

The author wishes to thank Dr. Tom Metzler at the Ball Aerospace communication systems Division, Broomfield, CO., U.S.A. for providing the data related to the plane-wave spectral method.

Appendix A

Let the infinite integration interval in (2) be truncated at $t=t_c$. Then the truncation error ϵ is (scale factor $\frac{\mu_1 k_1}{\pi^2}$ is omitted)

$$\epsilon = \int_{t_c}^{\infty} \frac{\sin^2(k_1 d \sqrt{\epsilon_r + t^2} t \sqrt{1+t^2} K_0(k_1 \rho t)}{(\epsilon_r + t^2) \cos^2(k_1 d \sqrt{\epsilon_r + t^2}) + (1+t^2) \sin^2(k_1 d \sqrt{\epsilon_r + t^2})} dt \quad (A.1)$$

Since $R_e(\epsilon_r) \gg I_m(\epsilon_r)$ in practice, the truncation error due to the imaginary part is in much lower order than that due to the real part alone. Hence, it is sufficient to estimate the truncation error assuming ϵ_r real. For ϵ_r real,

$$\epsilon \leq \int_{t_c}^{\infty} \frac{\sin^2(k_1 d \sqrt{\epsilon_r + t^2} t \sqrt{1+t^2} K_0(k_1 \rho t)}{1+t^2} dt$$

$$\begin{aligned} &\leq \int_{t_c}^{\infty} \frac{t}{\sqrt{1+t^2}} K_0(k_1 \rho t) dt \\ &\leq \int_{t_c}^{\infty} K_0(k_1 \rho t) dt \\ &\leq \frac{e^{-k_1 \rho t_c}}{k_1 \rho} \text{ for } k_1 \rho t_c \geq 0.7 \end{aligned} \quad (A.2)$$

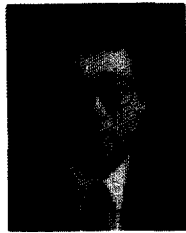
This analysis suggests that $t_c \approx \frac{1}{k_1 \rho} (\ln(10) - \ln(k_1 \rho))$ for a truncation error of 10^{-m} .

References

1. J.E. Rana and N.G. Alexopoulos, "Current Distribution and Input Impedance of Printed Dipoles," IEEE Trans. Antennas and Prop., Vol. AP-29, pp. 99-105, January 1981.
2. P.W. Hawkes, Ed., *Advances in Electronics and Electron Physics: A Dynamical Radiation Model for Microstrip structures.*, (by J.R. Mosig and F. E. Gardiol), Academic Press, 1982.
3. I.G. Choi, *An Efficient Representation for the Planar Microstrip Green's function.* Ph.d. Dissertation,

The Ohio State University, September 1986.

4. L.B. Felson and N. Marcuvitz, *Radiation and Scattering of Waves*, Prentice-Hall, New Jersey, 1973.
5. R.E. Collin, *Field Theory of Guided Waves*, McGraw Hill, New York, 1960.
6. D.M. Pozar, "Input Impedance and Mutual Coupling of Rectangular Microstrip antennas," IEEE Trans. Antennas and Prop., Vol. AP-30, pp. 1191-1196, November 1982.
7. N.K. Uzunoglu, N.G. Alexopoulos, and J.G. Fikioris, "Radiation Properties of Microstrip dipoles," IEEE Trans. Antennas and Prop., Vol. AP-26, pp. 853-858, November 1979.
8. D.R. Jackson and N.G. Alexopoulos, "An Asymptotic Extraction Technique for Evaluating Sommerfeld-Type Integrals," IEEE Trans. Antennas and Prop., Vol. AP-34, pp. 1467-1470, December 1986.



崔翼權 (Ik Guen Choi) 정회원

1950년 12월 26일생

1974년 2월: 서울대학교 공과대학
자원공학과(공학사)

1976년 2월: 서울대학교 대학원 자
원공학과(공학석사)

1986년 9월: 미국 오하이오주립대
학교 대학원 전자공학
과(공학박사)

1976년 3월 ~ 1979년 6월: 육군 제3사관학교 교수부 물리
학 전임강사

1981년 10월 ~ 1986년 9월: 미국 오하이오주립대학교 ESL
(Electro Science Laboratory)
연구원

- 지하구조물 탐사용 레이다시스템개발연구

- 마이크로스트립 어레이 안테나개발연구

1986년 10월 ~ 1987년 9월: 미국 마사추세츠주립대학교
Antenna Laboratory 연구원

- 마이크로스트립 웨이스트 어레이 안테나
연구

1987년 10월 ~ 현재: 한국 전자통신연구소 이동통신기술연
구부

- 위성추적레이다 시스템 성능분석연구

- 식별후보자동 송출 및 수신시스템 개발연
구

- 특수 페이지개발연구

- 이동통신용 소형내장형안테나개발 및 진
파특성연구

- EMI / EMC 측정 및 방지대책연구